INSTITUTE OF PHYSICS PUBLISHING JOURNAL OF PHYSICS A: MATHEMATICAL AND GENERAL

J. Phys. A: Math. Gen. **39** (2006) 4527–4531 doi:10.1088/0305-4470/39/17/S33

Screened Coulomb balls—structural properties and melting behaviour

V Golubnychiy[1], H Baumgartner[1], M Bonitz[1], A Filinov[1] and H Fehske[2]

[1] Christian-Albrechts-Universität Kiel, Institut für Theoretische Physik und Astrophysik, 24098 Kiel, Germany
[2] Universität Greifswald, Institut für Physik, l7487 Greifswald, Germany

Received 9 September 2005, in final form 6 November 2005
Published 7 April 2006
Online at stacks.iop.org/JPhysA/39/4527

Abstract
Classical molecular dynamics and Monte Carlo simulations are used to investigate three-dimensional spherical charged particle clusters which were experimentally observed in dusty plasmas (Arp *et al* 2004 *Phys. Rev. Lett.* **93** 165005). The shell configuration and geometry of the ground state is found to change with the screening parameter. The melting temperature of small clusters exhibits a non-monotonic dependence on the total number of particles.

PACS numbers: 52.27.Lw, 52.27.Gr

Introduction

Since their first experimental observation [1, 2], two-dimensional (2D) crystals of dust particles in an external potential continue to be of large interest, see e.g. [3, 4] for an overview. Recently, experiments with three-dimensional (3D) dust clusters were reported [5] indicating that the interaction between the particles is screened [6]. This contribution deals with a theoretical analysis of small spherical 3D crystals with screened Coulomb interaction in a parabolic confinement and with the investigation of their melting behaviour by using classical molecular dynamics (MD) and Monte Carlo (MC) simulations.

Structural changes of the ground state of Yukawa clusters

We consider N classical particles with equal charge q in a 3D isotropic parabolic trap with frequency ω_0 described by the Hamilton function

$$H_N = \sum_{i=1}^{N} \frac{m}{2}\dot{r}_i^2 + \sum_{i=1}^{N} \frac{m}{2}\omega_0^2 r_i^2 + \sum_{i>j}^{N} \frac{q^2}{4\pi\varepsilon r_{ij}} \mathrm{e}^{-\kappa r_{ij}}, \tag{1}$$

where κ is the screening parameter and $r_{ij} = |\mathbf{r}_i - \mathbf{r}_j|$. Below we will use dimensionless lengths and energies by introducing $r_0 = (q^2/2\pi\varepsilon m\omega^2)^{1/3}$ and $E_0 = (m\omega^2 q^4/32\pi^2\varepsilon^2)^{1/3}$.

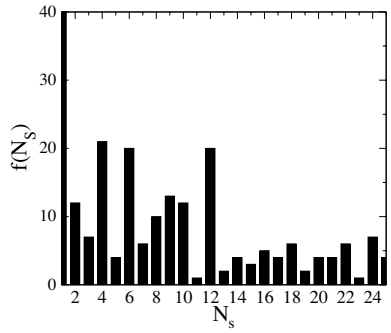

Figure 1. Total frequency of occurrence of shells containing N_S particles for all Coulomb clusters (ground state configurations) with $N = 2, \ldots, 160$.

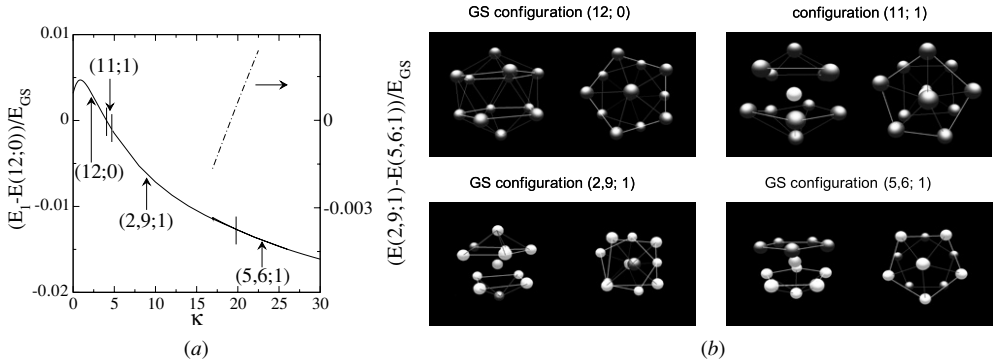

(*a*) (*b*)

Figure 2. (*a*) Energy difference between the two configurations with one particle in the centre (E_1) and no particle in the centre ($E(12; 0)$) of the cluster $N = 12$ divided by the GS energy as a function of screening parameter. With increasing κ the geometry of the former changes from (11;1) to (2, 9; 1) and later to (5, 6; 1). Dash-dotted line shows energy difference of the configurations (2, 9; 1) and (5, 6; 1), right axis. Arrows indicate the ground state configuration, short vertical lines the transition points. (*b*) Frontview (left part of each panel) and view from below (right part) for the possible configurations of the cluster with $N = 12$, see text.

The length r_0 is the stable distance of two particles confined in the considered potential in the case of zero screening, and E_0 denotes their ground state energy. To investigate the influence of screening on the ground state (GS) and metastable state (MS), we combine classical MD and simulated annealing methods [8].

Previous investigations [7–10] characterized the relative stability of different clusters in terms of binding energies and shell symmetry. Another interesting quantity is the frequency of occurrence of shells with given particle number N_S for all clusters with $N = 2, \ldots, 160$ which is shown in figure 1, where we counted the total number of clusters containing N_S particles on any shells. The peaks at $N_S = 4, 6, 12$ indicate particularly stable configurations while, e.g. configurations with $N_S = 11, 23$ are only seen once and therefore are relatively unstable. The (in)stability is also relevant for melting of such clusters which will be discussed below.

Next we consider the dependence of the GS configuration on κ for a cluster with $N = 12$. The energy difference between the energetically lowest configurations is shown in figure 2(*a*). The unscreened system has the GS $(12; 0)$, i.e. all particles are located on a single shell,

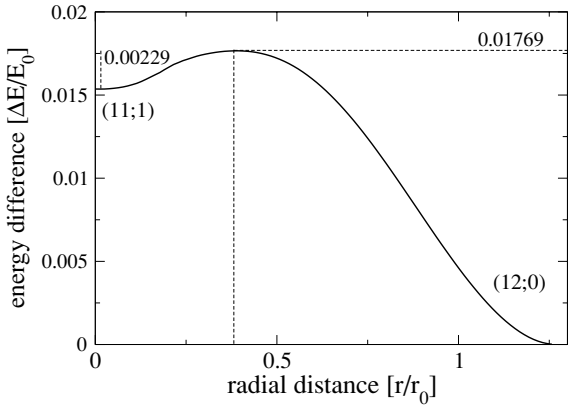

Figure 3. Energy increase in the Coulomb ball for $N = 12$ and $\kappa = 0$, when one particle is moved from the shell (GS) towards the centre (metastable configuration) while relaxing the configuration of the remaining particles. The maximum of ΔE yields the potential barrier for inter-shell transitions.

whereas the first excited state configuration is (11; 1), i.e. one particle is in the centre. The GS changes to configuration (11; 1) at a critical value of $\kappa = 4.1$. Furthermore, at $\kappa = 4.7$, the shell with 11 particles splits into two subshells (2, 9) with slightly different radii. Finally, at $\kappa = 19.1$, the subshell configuration changes to (5, 6; 1) which remains the GS for all larger values of κ. These configurations are shown in figure 2(*b*). In the front view of the GS configuration (5, 6; 1), the trend towards formation of layers at large κ can be seen. The observation of increased shell population of the inner shells with higher screening and the splitting into subshells is found to be a general trend for screened Coulomb balls.

Melting behaviour of small unscreened Coulomb clusters

In order to analyse the melting behaviour of these small clusters, we have performed classical MC simulations in the canonical ensemble up to particle numbers of $N = 100$ [11]. For low temperature, the same GS and MS states as in the MD simulation are reproduced. Consider now the melting behaviour at finite temperature of the heat bath T. It turns out that at low temperature, first intra-shell melting is observed (connected with a change of the symmetry within a given shell). At larger temperature we observe inter-shell melting, in agreement with [12], similar to the behaviour of two-dimensional Coulomb clusters [13].

As an example of the latter we plot in figure 3 the potential barrier for a cluster with $N = 12$ between the configurations (12; 0) and (11; 1). The potential barrier from the GS configuration (12; 0) to the potential maximum is about an order of magnitude higher than the potential barrier for the excited state (11; 1) reflecting the different relative stability of the two states. Furthermore, the ratio of these barriers is found to be proportional to the ratio of the melting temperatures, see figure 4(*a*). We obtain the melting temperature from an analysis of the relative distance fluctuations [13]

$$u_r = \frac{2}{N(N-1)} \sum_{i<j}^{N} \sqrt{\langle r_{ij}^2 \rangle / \langle r_{ij} \rangle^2 - 1},$$

which are found to be sensitive to melting in such mesoscopic clusters.

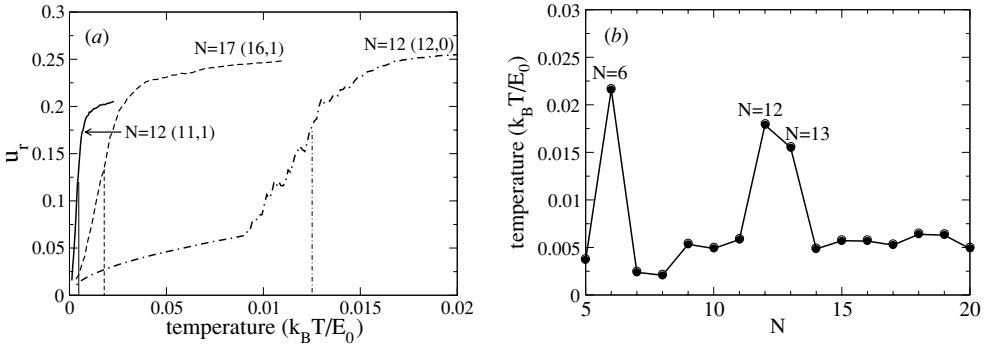

Figure 4. Inter-shell melting behaviour of small unscreened Coulomb balls. (*a*) Relative distance fluctuations for Coulomb balls with the configurations (12; 0), (11; 1) and (16; 1). (*b*) Melting temperature versus total particle number (the line is a guide for the eye).

From figure 4(*a*), we observe that the melting of the magic cluster with $N = 12$ (in the GS configuration) occurs at significantly higher temperature than for the cluster $N = 17$. This difference of the melting temperatures, cf figure 4(*b*), is in agreement with the analysis of the structural properties of small clusters, such as the binding energies and cluster symmetry, cf. [8, 9] and references therein. This behaviour is representative for spherical 3D Coulomb balls in general and also for screened Coulomb balls. A more general analysis of the influence of screening on the melting behaviour is given in [6].

Relation to spherical dust crystals

The present model (1) is directly applicable to ion crystals (for $\kappa = 0$) and dust Coulomb balls [5]. In the latter case, the plasma properties enter the model via the Debye screening parameter $\kappa \to 1/r_D$, and the temperature in the melting analysis refers to the dust particle temperature. The model (1) is able to correctly reproduce the shell configurations of the experiment, for details see [6]. In contrast, the recent theoretical model of [14] predicts approximately screening independent shell populations which differ from the measurements [5, 6].

Acknowledgments

This work is supported by the Deutsche Forschungsgemeinschaft via SFB-TR 24 grants A5 and A7. We acknowledge discussions with D Block, W D Kraeft, P Ludwig and A Piel.

References

[1] Thomas H, Morfill G E, Demmel V, Goree J, Feuerbacher B and Mölmann D 1994 *Phys. Rev. Lett.* **73** 1529
[2] Hayashi Y and Tachibana K 1994 *Japan. J. Appl. Phys.* **33** L804
[3] Morfill G E and Kersten H (eds) 2003 Focus on complex (dusty) plasmas *New J. Phys.* **5**
[4] Dubin D H E and O'Neill T M 1999 *Rev. Mod. Phys.* **71** 87
[5] Arp O, Block D, Melzer A and Piel A 2004 *Phys. Rev. Lett.* **93** 165004
[6] Bonitz M *et al* 2005 *Preprint* physics/0508212 submitted
[7] Hasse R W and Avilov V V 1991 *Phys. Rev.* A **44** 4506
[8] Ludwig P, Kosse S and Bonitz M 2005 *Phys. Rev.* E **71** 046403

[9] Arp O, Block D, Bonitz M, Fehske H, Golubnychiy V, Kosse S, Ludwig P, Melzer A and Piel A 2005 *J. Phys: Conf. Ser.* **11** 234
[10] Tsuruta K and Ichimaru S 1993 *Phys. Rev.* A **48** 1339
[11] For an analysis of larger clusters see Schiffer J P 2002 *Phys. Rev. Lett.* **88** 205003
[12] Dubin D H E and O'Neil T M 1988 *Phys. Rev. Lett.* **60** 511
[13] Filinov A V, Bonitz M and Lozovik Yu E 2001 *Phys. Rev. Lett.* **86** 3851
[14] Totsuji H, Ogawa T, Totsuji C and Tsuruta K 2005 *Phys. Rev.* E **72** 036406